pH Dependence Thermal Stability of a Chymotrypsin Inhibitor from *Schizolobium parahyba* Seeds

Rozeni C. L. Teles,* Leonardo de A. Calderon,* Francisco J. Medrano,† João A. R. G. Barbosa,† Beatriz G. Guimarães,† Marcelo M. Santoro,‡ and Sonia M. de Freitas*

*Universidade de Brasília, Depto Biologia Celular, Laboratório de Biofísica, Brasilia DF, Brazil, 70910-900; †Centro de Biologia Molecular Estrutural-Laboratório Nacional de Luz Síncrotron (CeBiME-LNLS) Campinas, SP, Brazil; and ‡Universidade Federal de Minas Gerais, Depto Bioquímica e Imunologia, Belo-Horizonte, MG, Brazil

ABSTRACT The thermal stability of a *Schizolobium parahyba* chymotrypsin inhibitor (SPCI) as a function of pH has been investigated using fluorescence, circular dichroism, and differential scanning calorimetry (DSC). The thermodynamic parameters derived from all methods are remarkably similar and strongly suggest the high stability of SPCI under a wide range of pH. The transition temperature (T_m) values ranging from 57 to 85.3°C at acidic, neutral, and alkaline pH are in good agreement with proteins from mesophilic and thermophilic organisms and corroborate previous data regarding the thermal stability of SPCI. All methods gave transitions curves adequately fitted to a two-state model of the unfolding process as judged by the cooperative ratio between the van't Hoff and the calorimetric enthalpy energies close to unity in all of the pH conditions analyzed, except at pH 3.0. Thermodynamic analysis using all these methods reveals that SPCI is thermally a highly stable protein, over the wide range of pH from 3.0 to 8.8, exhibiting high stability in the pH region of 5.0–7.0. The corresponding maximum stabilities, ΔG^{25}, were obtained at pH 7.0 with values of 15.4 kcal mol^{-1} (combined fluorescence and circular dichroism data), and 15.1 kcal mol^{-1} (DSC), considering a ΔC_p of 1.72 ± 0.24 kcal mol^{-1} K^{-1}. The low histidine content (~1.7%) and the high acidic residue content (~22.5%) suggests a flat pH dependence of thermal stability in the region 2.0–8.8 and that the decrease in thermal stability at low pH can be due to the differences in *pK* values of the acidic groups.

INTRODUCTION

Protein stability can be measured directly using calorimetric methods, and indirectly by the Gibbs energy change estimated from transition curves of native to the unfolded state (Privalov, 1979; Pace, 1990). In many cases the folding of proteins is a cooperative process, in which only the native (N) and the unfolded (U) states are present in equilibrium (Kumar et al., 2003). A conformational transition between these two states is generally observed for small proteins with only one domain. In the folding process all molecules can be considered to exist in either one of these two structural states or in an intermediary one. Many proteins, under weak denaturing conditions, can adopt this structurally intermediate form, resembling more the native state than the unfolded state (Ptitsyn and Uversky, 1994). The elucidation of the nature of these transitions and the existence or not of folding intermediates is a prerequisite for the kinetic and thermodynamic analysis of the unfolding process (Arnold and Ulbrich-Hofmann, 1997).

Protease inhibitors have potential for the regulation of proteolytic activities in specific pathways (Laskowski and Kato, 1980; Bode and Huber, 2000). Overall, protease inhibitors can be taken as models for inhibition of proteolytic enzymes, especially those that are usually responsible for animal and microorganism digestion (Richardson, 1977). Serine proteases of the chymotrypsin and subtilisin families and their natural protein inhibitors are among the most widely studied models of protein-protein recognition (Otlewski et al., 1999; Ascenzi et al, 2003).

Serine protease inhibitors are the best-known and most characterized inhibitors. They are classified into 18 different families, based on the amino acid sequence, structural similarities, and mechanism of reaction with their respective enzymes (Laskowski and Qasim, 2000). Two main inhibitor families from leguminous plants have been characterized and they are known as Kunitz- and Bowman-Birk-type protease inhibitors (Laskowski and Kato, 1980; Valueva and Mosolov, 1999). These inhibitors have been described as protective agents against the attack of insects and pathogenic microorganisms (Ryan, 1990; Broadway, 1995; Wilson and Chen, 1983; Shukle and Wu, 2003). For this reason, transgenic plants expressing these protease inhibitors have been tested for enhanced defensive properties against insect pests (Hilder and Boulter, 1999; Schuler et al., 1998; Franco et al., 2003). They share a common main-chain conformation at the binding loop, which is maintained throughout most of the inhibitor families, despite lack of similarity in the rest of the protein (Otlewski et al., 2001). Kunitz-type inhibitors have been characterized with respect to their evolutive (Pritchard and Dufton, 1999) and structural aspects, but there are few studies about the stability of these inhibitors. In one of these, thermal denaturation of the soybean trypsin inhibitor was studied using high-sensitivity differential scanning calorimetry (DSC) to determine the pH-dependence of protein stability (Grinberg et al., 2000; Burova et al., 2002). The thermal

Submitted May 27, 2004, and accepted for publication February 4, 2005.

Address reprint requests to Sonia M. de Freitas, E-mail: nina@unb.br.

0006-3495/05/05/3509/09 $2.00

doi: 10.1529/biophysj.104.045682

denaturation of this protein, at the pH range 2.0–11.0, has been described as a two-state model (Varfolomeeva et al., 1989). Indeed, the main representative member of Kunitz-type inhibitor, the bovine pancreatic trypsin inhibitor, is one of the most extensively structurally studied (Otlewski et al., 2001; Makhatadze et al., 1993).

Schizolobium parahyba chymotrypsin inhibitor (SPCI) is a Kunitz-type inhibitor with a single polypeptide chain, presenting four cysteine residues linked into two disulfide bonds (Souza et al., 1995; Teles et al., 2004). It suppresses the proteolytic activity of chymotrypsin through the formation of a stable complex with a 1:1 stoichiometry. The secondary structure of SPCI is mainly formed by β-strands and unordered structures (Teles et al., 1999), and its native structure is mainly maintained by hydrophobic forces and electrostatic interactions (Souza et al., 2000). The molecular arrangements of SPCI at pH 7.0, visualized by atomic force microscopy at high resolution in nanopure water, indicated an organization in different oligomeric states, with predominance of hexagonal forms (Leite et al., 2002).

Currently, the research about protease inhibitors is driven by their potential applications in medicine, agriculture, and biotechnology. In this context, the determination of the physicochemical parameters characterizing the structural stability of the inhibitors is essential to select effective and stable inhibitors under a large variety of environmental conditions. Moreover, the knowledge of their structural features is fundamental to understand the inhibitor-enzyme interactions and allow novel approaches in the use of synthetic inhibitors aiming for drug design.

Protease inhibitors are widely distributed in plant seeds, where they act as anti-nutritional agents, especially in insects where they inhibit midgut proteases. They also inhibit a broad spectrum of activities including suppression of pathogenic nematodes and growth inhibition of many pathogenic fungi (Joshi et al., 1998). Kunitz-type inhibitors have been reported to have the potential to suppress ovarian cancer cell invasion and peritoneal disseminated metastasis in vivo (Kobayashi et al., 2004). In addition, Kunitz-type inhibitors had an adverse effect on insect development and might serve as a transgenic resistance factor (Shukle and Wu, 2003). These advantages make protease inhibitors an ideal choice to be used in biotechnological applications, especially in developing transgenic crops resistant to insect pests.

Although the major digestive protease in the midgut of insects are serine proteases with trypsin-like and chymotrypsin-like specificity (Bown et al., 1997), the proteases showed differences from bovine enzymes with respect to their interaction with the plant protease inhibitors. Therefore, to achieve an effective pest control strategy, it is very important to select different inhibitors presenting high stability under different conditions and to know the feature of midgut proteases, as well as the effects of the inhibitors on their activities. In this work, we present the characterization of the pH dependence on SPCI thermal stability, to establish the ideal conditions for further biotechnological applications in developing transgenic crops resistant to insect pests. Furthermore, structural analysis would greatly help in enzyme and SPCI engineering to more potent forms, against certain targeted pest species. These studies would be performed with the elucidation of the three-dimensional structure of SPCI that was recently crystallized. The x-ray data collection and structure determination are in progress at Brazilian Synchrotron Light Laboratory (J. A. R. G. Barbosa, R. C. L. Teles, and S. M. de Freitas, unpublished data).

MATERIALS AND METHODS

Protein purification

SPCI was purified from *Schizolobium parahyba* seeds as previously described (Teles et al., 2004). Concentration of SPCI was determined spectrophotometrically using the absorption coefficient of $A^{\%}_{280} = 6.18$ (Souza et al., 1995).

Fluorescence spectroscopy

Fluorescence measurements were carried out using a JASCO (Easton, MD) FP-777 fluorescence spectrometer. Spectra were recorded from 300 to 400 nm using an excitation wavelength of 280 nm, and 5 nm bandwidth for both excitation and emission. To measure the temperature dependence of the protein emission fluorescence, solutions containing 8 μM of SPCI in 50 mM 3-(*N*-morpholino propane sulfonic acid) (MOPS) pH 7.0 buffer at pH 7.0 were equilibrated for 15 min in a 1.0 $\times$ 1.0-cm cuvette into a thermostated cell holder using a Peltier-type temperature controller at temperatures ranging from 25 to 110°C. Data were analyzed by assuming a two-state transition considering the changes in emission fluorescence intensities at 336 nm. To correct for the effect of the temperature on the fluorescence intensities, data were normalized taking into account the recorded emission of *N*-acetyl-L-tryptophanamide (NATA) under identical conditions to the protein experiments and at the same molar concentration of tryptophan residue in SPCI (Richardson et al., 2000). The protein fraction present in the unfolded conformation (f_U), equilibrium constant (K_{eq}), and Gibbs free energy were calculated using the following equations:

$$f_U = (y_F - y)/(y_F - y_U) \quad (1)$$

$$K_{eq} = [U]/[N] = f_U/(1 - f_U) \quad (2)$$

$$\Delta G = -RT \ln K_{eq} = -RT \ln [(y_F - y)/(y - y_U)], \quad (3)$$

where y_F and y_U represent the amount of y in the folded and unfolded states, respectively. These data were fitted according to Eq. 4 considering the van't Hoff approximation (Eq. 5):

$$Yobs = \frac{(Yd + Md \times T) \times \exp((\Delta S/R) - (\Delta H/RT)) + (Yn + Mn \times T)}{1 + \exp((\Delta S/R) - (\Delta H/RT))} \quad (4)$$

$$Ln\,K_{eq} = (\Delta S/R) - (\Delta H/R)(1/T), \quad (5)$$

where K_{eq} is the experimentally observed equilibrium constant, T is temperature in Kelvin (K), ΔH is the slope from the fitted regression (the van't Hoff change in enthalpy), and ΔS is the intersection from the fitted regression (the change in entropy). In Eq. 4, these parameters have the same meaning. Additionally, *Yn* and *Mn* represent the intercept and slope of the pretransition straight line, respectively, whereas *Yd* and *Md* represent the intercept and slope of the posttransition straight line, repectively.

The correspondent stability at 25°C (ΔG^{25}) was estimated from the Gibbs-Helmholtz equation (Eq. 6), considering the temperature range where unfolding occurs:

$$\Delta G_{(T)} = \Delta H_m(1 - T/T_m) - \Delta C_p[(T_m - T) + T\ln(T/T_m)]. \quad (6)$$

ΔC_p is the change in heat capacity that accompanies protein unfolding. For SPCI, ΔC_p was calculated from DSC transitions using the linear representation of ΔH versus temperature (Privalov and Potekhin, 1986). The temperature of maximum stability (T_{max}) was calculated using Eq. 7:

$$T_{max} = T_m/\{\exp[\Delta H_m/(\Delta C_p T_m)]\}. \quad (7)$$

Circular dichroism spectroscopy

Circular dichroism (CD) measurements were carried out on a JASCO J-810 spectropolarimeter, equipped with a Peltier-type temperature controller, and a thermostated cell holder, interfaced with a thermostatic bath. Spectra were recorded in 0.1-cm pathlength quartz cells at a protein concentration of 0.15–0.20 mg/ml in 50 mM citrate-phosphate buffer at pH 3.0, 50 mM Na-acetate buffer at pH 4.2, 50 mM MOPS buffer at pH 7.0, and 50 mM Tris-HCl buffer at pH 8.8. Five consecutive scans were accumulated and the average spectra stored. Thermal denaturation experiments were performed by increasing the temperature from 20 to 95°C, allowing temperature equilibration for 5 min before recording each spectrum. The observed ellipticities were converted into the mean residue ellipticities [θ] based on a mean molecular mass per residue of 112 Da. The data were corrected for the baseline contribution of the buffer and the observed ellipticities at 225 nm were recorded. Thermodynamic parameters derived from transition curves were calculated in the same way as the fluorescence measurements. The temperature dependence of the secondary structure was estimated from fitted far-ultraviolet CD curves (Bolotina and Lugauskas, 1985; Bolotina, 1987).

Differential scanning calorimetry

The apparent specific heat capacity of SPCI as a function of temperature was obtained in a VP-DSC (Microcal, Northampton, MA) at scan rate of 1.0°C min^{-1}. Protein sample was prepared by dissolving lyophilized SPCI in 50 mM MOPS buffer at pH 7.0 or 50 mM sodium citrate buffer at pH 2.0–5.0, followed by centrifugation at 8000 × *g* for 15 min. This solution was degassed before it was loaded into the DSC cells. A blank scan with buffer in both calorimeter cells was subtracted automatically to correct for differences between the cells. Consecutive scans were performed to demonstrate reversibility. The influence of the irreversible steps on the heat capacity curves was checked by running samples at several scanning rates (0.2, 0.75, and 1.0°C min^{-1}).

Data were analyzed using the routines of Origin software (version 4.0, MicroCal) to obtain the temperature at the midpoint of the unfolding transition (T_m), the calorimetric (ΔH_{cal}), and the van't Hoff enthalpy energy of denaturation (ΔH_{vh}). A baseline between the pre- and posttransition regions was subtracted from the endotherm to calculate the area, which is equal to the unfolding calorimetric enthalpy. The corresponding van't Hoff enthalpy energy was estimated using the following equation:

$$\Delta H_{vh} = 4RT_m^2 C_{p,max}/\Delta H_{cal}, \quad (8)$$

where $C_{p,max}$ represents the maximum peak height to the area of the transition, and T_m is the temperature at $C_{p,max}$. The cooperative ratio (*CR*) is defined by the relation: $CR = \Delta H_{vh} / \Delta H_{cal}$ and used to estimate the number of steps in the unfolding process.

RESULTS AND DISCUSSION

Heat-induced unfolding fluorescence analysis

Fluorescence has been an important method to study protein conformation because it reflects the environment-dependent solvent exposure of the tryptophan indole ring and the tyrosine aromatic side chain (Eftink, 1994; Eftink and Shastry, 1997). The transition curve from heat-induced fluorescence emission changes of SPCI at pH 7.0, fitted according to Eq. 4, is shown in Fig. 1. The decrease in intrinsic tryptophan fluorescence emission was recorded after incubation of SPCI at different temperatures for 15 min to establish the equilibrium between native and unfolded protein forms. The fluorescence intensities of NATA were considered to avoid ambiguity in the estimation of the temperature-dependence fluorescence corresponding to the native and unfolded states (Richardson et al., 2000). Therefore, the thermally induced decrease in fluorescence emission is only due to the solvent exposure of tryptophan residue in SPCI reflecting changes in the environment of its side chain.

Experimental curves from the different measurements of fluorescence emission at 336 nm were considered to deter-

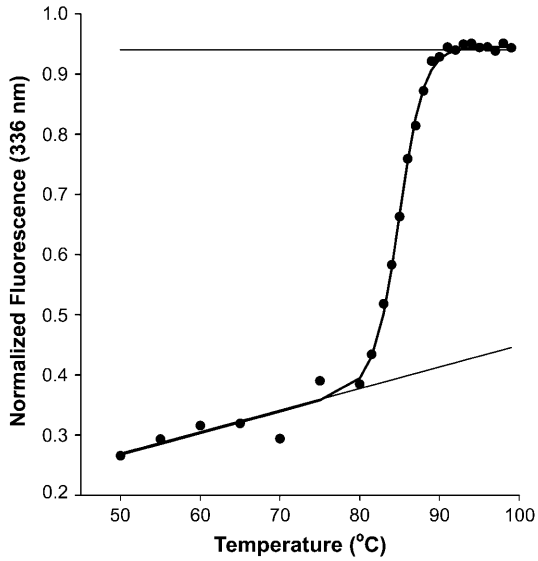

FIGURE 1 Temperature-induced unfolding profile of SPCI at pH 7.0 monitored by changes in tryptophan fluorescence intensity at 336 nm. The temperature-dependence transition curve was calculated from the ratio of fluorescence intensities of SPCI and NATA at the same concentration as that of tryptophan in SPCI measurements. These data were used to obtain the fitted curve by nonlinear regression according to Eq. 4 (see Materials and Methods). Table 1 shows the thermodynamic parameters derived from combined fluorescence and circular dichroism data.

mine the fractions F_u for each temperature (Fig. 1). Because the shape of the transition curve is characteristic of an apparent cooperative process, the data were analyzed assuming a two-state temperature-induced unfolding as a function of pH fitted as a nonlinear extrapolation (Santoro and Bolen, 1992), according to the van't Hoff approximation.

The temperature at which half of the protein is unfolded (T_m), the unfolding enthalpy change at T_m (ΔH_m) calculated from the fluorescence fitted unfolding curve according to Eq. 4, and the correspondent stability at 25°C (ΔG^{25}) are 84.8°C, ~160.0 ± 3.0 kcal mol^{-1}, and ~17.0 ± 2.5 kcal mol^{-1}, respectively. These thermodynamic parameters are slightly different from those obtained from circular dichroism due the experimental difficulty of highly cooperative transitions for both techniques. However, these parameters calculated from fluorescence and CD combined data at pH 7.0 were similar to those obtained from DSC (Tables 1 and 2). For most naturally occurring globular proteins the conformational stability is between 5 and 15 kcal mol^{-1} (Pace, 1990). The unfolding enthalpy change of 145 ± 6 kcal.mol^{-1}, T_m of 84.9°C, and ΔG^{25} of 15.4 ± 2.1 kcal mol^{-1}, obtained by nonlinear fitting of Eq. 4 to the combined fluorescence and CD data at pH 7.0, show that SPCI is a highly thermostable protein.

Heat-induced unfolding CD analysis

Far-UV CD is one of the most sensitive physical techniques for analyzing secondary structure and monitoring structural changes occurring in proteins (Yang et al., 1986; Venyaminov et al., 1996). Fig. 2 presents far-UV CD spectra at pH 7.0 recorded in the temperature range of 20–90°C. The secondary structure content (Bolotina, 1987) (Fig. 2, *inset*) mainly shows a significant decrease in β-structure content, but part of the secondary structure is still preserved at 90°C. Between 20 and 70°C the CD spectra is typical of β-structure and unordered structure proteins (Fig. 2, *inset*). These results are in agreement with those previously reported for SPCI using Raman and FTIR spectroscopy in which the secondary structure was mainly characterized as β-strands and unordered structures at pH 7.0 (Teles et al., 1999). At temperatures above 70°C the CD spectra decrease the minimum at 200 nm with a partial loss of the signal. Analysis of the temperature progress curve at pH 7.0 (Fig. 2) reveals that the native conformation of SPCI is thermally stable at temperatures below 70°C with partial unfolding of <6% of its secondary elements (Fig. 2, *inset*). The secondary structure is only perturbed upon heating from 70 to 90°C. These results indicate compensation between an increase of ~10 percentage points (3–13%) in α-helix and a decrease of ~36 percentage points (75–39%) in β-turn and the total disruption of β-sheet content (18–1%).

These results suggest that the thermal treatment of SPCI up to 90°C was not enough to produce complete unfolding of the protein. As we previously demonstrated, the inhibitory activity of SPCI toward chymotrypsin remained unaffected even after incubation at 70°C for 1.0 h at pH 7.6. However, SPCI lost 25% of its inhibitory activity at 80°C for 1.0 h and 50% at 90°C in ~3 h at pH 7.6 (Souza et al., 2000). In fact, SPCI was only completely inactivated by heating at 90°C, or in the presence of 8 M urea, high ionic strength (1 M KCl), or 20% PEG (w/v). The complete denaturation of SPCI was observed in transition curves at the temperature range of 20–93°C, with a transition temperature of unfolding (T_m) equal to or above 74.9°C in all analyzed pH conditions (Fig. 3 and

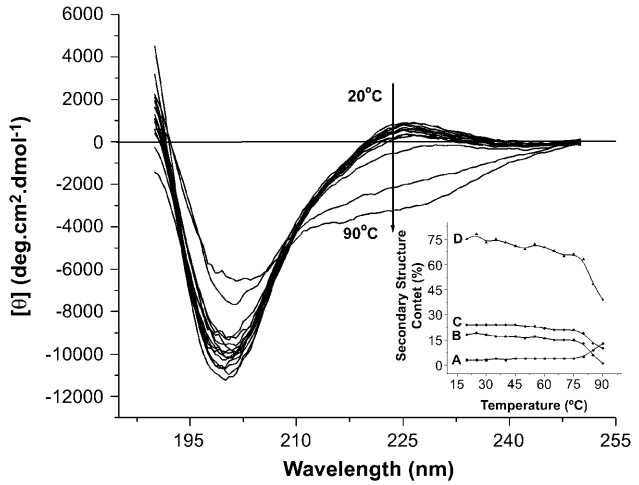

FIGURE 2 Far-UV CD spectra of SPCI at pH 7.0, as a function of temperature ranging from 20 to 90°C. The secondary structure contents were estimated from these spectra and are presented in the inset as follows: (*A*) α-helix; (*B*) β-sheet; (*C*) others; and (*D*) β-turn content as a function of temperature. The ellipticities at 225 nm were considered to obtain the curve presented in Figs. 3 and 7.

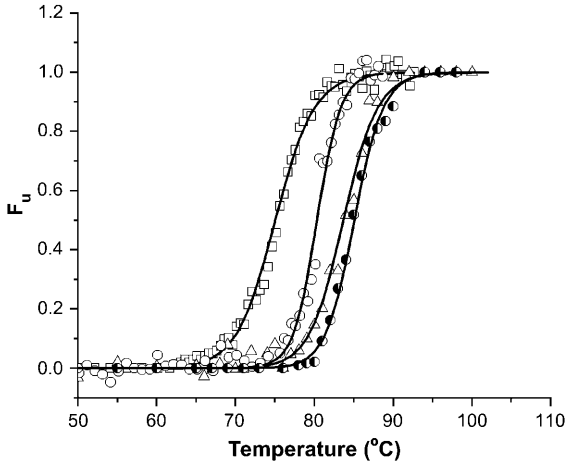

FIGURE 3 Fitted heat-induced unfolding curves of SPCI according to Eq. 4 (see Materials and Methods), obtained at pH 3.0 (*open squares*), 4.2 (*open triangles*), 7.0 (*half-solid circles*), and 8.8 (*open circles*). These data are calculated considering the change in ellipticities at 225 nm. The estimated thermodynamic parameters derived from these analyses are presented in Table 1.

TABLE 1 Thermodynamic parameters for the thermal unfolding of SPCI obtained from fluorescence and far-UV CD measurements at different pH values

pH	T_m°C	(ΔH_m kcal mol^{-1})	(ΔS_m cal mol^{-1} K^{-1})	(ΔG^{25} kcal mol^{-1})
		Combined CD and fluorescence		
7.0	84.9	145 ± 6	406 ± 17	15.4 ± 2.1
		Circular dichroism		
3.0	74.9	101 ± 13	290 ± 38	8.0 ± 1.5
7.0	84.9	131 ± 23	367 ± 65	13.0 ± 2.9
8.8	83.5	125 ± 25	352 ± 69	11.7 ± 2.9

Table 1). The temperature from 94 to 98°C was extrapolated from the fitted transition curves.

The unfolding process induced by increasing the temperature was monitored following the ellipticity at 225 nm as shown in Fig. 3 (pH 3.0, 4.2, 7.0, and 8.8). A sigmoid dependence of the ellipticity with the temperature was observed with practically no change for the native SPCI until 70°C. However, after this point, a large change in ellipticity and a decrease in the intensity of the signal were observed, suggesting unfolding but no complete disruption of the secondary structure up to 93°C (Fig. 2). According to calorimetric assays the complete unfolding of SPCI occurs at temperatures over 93°C. These results were similar with T_m obtained by the change of emission intensity at 336 nm (Fig. 1) at pH 7.0.

The transition temperatures around 85°C obtained at pH 7.0 by all methods suggest that SPCI has a melting temperature characteristic of thermally stable proteins (Table 1) at neutral pH. The agreement between combined fluorescence and CD data (Fig. 7) indicates that the side-chain conformational changes accompany changes in the secondary structure of SPCI. These thermodynamic analyses reveals that SPCI is a highly stable protein at neutral pH, exhibiting a ΔG^{25} of 15.4 ± 2.1 kcal mol^{-1} and the corresponding temperature of maximum stability (T_{max}) of 10°C, calculated from Eqs. 6 and 7, respectively. T_{max} is in agreement with other globular proteins that are predicted to have maximum stability between −10 and +35°C (Pace, 1990; Kumar et al., 2003; Tsonev and Hirsh, 2000; Ganesh et al., 1999; Zweifel and Barrick, 2002).

Far-UV CD was used to monitor the unfolding of SPCI at pH 3.0, 4.2, 7.0, and 8.8 (Fig. 3). The thermodynamic parameters are presented in Table 1. There are significant differences in these parameters at pH 3.0, where SPCI presents lower thermal stability when compared to pH 4.2 (data not shown), 7.0, and 8.8. The transition curve at pH 4.2 revealed the tendency of SPCI to precipitate at high temperature (>95%) leading to a not-well-defined posttransition baseline. Despite that, the thermodynamic parameters calculated from the fitted curve at pH 4.2 were compatible with the maximum stability of SPCI matching pH = *pI* (T_m = 85°C; $\Delta H \sim 165$ kcal mol^{-1}; $\Delta G^{25} \sim$ 18–20 kcal mol^{-1}). However, to conclude anything about the high stability of SPCI close to the *pI*, it is necessary to develop unfolding assays that could avoid the aggregation of the protein at pH values close to the *pI*.

DSC analysis

The calorimetric method is best suited to analyze the thermal unfolding transitions of proteins. The importance of this method relates to its ability to provide a direct energetic description of protein unfolding (Privalov, 1979). When protein denaturation occurs via a two-state mechanism, the ratio of the calorimetric enthalpy change obtained from the isotherms and the van't Hoff enthalpy change is equal or close to unity. The experimentally measured enthalpy change of protein unfolding represents the sum of the enthalpies associated with hydration of apolar and polar groups exposed to water upon unfolding, disruption of the van der Waals interactions between polar groups, disruption of hydrogen bonds, and the number of hydrogen bonds (Privalov and Makhatadze, 1992, 1993).

Data of the partial molar heat capacity at acidic and neutral pH for the unfolding of SPCI are shown in Fig. 4. The heat capacity profiles were found to be independent of the scan rate (data not shown). Therefore, the kinetic control of the denaturation processes can be discarded, and the thermodynamic analysis of DSC curves is justified. The thermal unfolding of SPCI at acidic conditions is a reversible process, as demonstrated by rescanning the sample (five rescans) after complete thermal denaturation up to 100°C, returning from the posttransitional baseline (data not shown). However, at pH 7.0, the reversibility was ~95% once the rescan of the sample was done up to 95°C because the tendency of SPCI to aggregate in this condition. It is known that upon heating the protein, the solubility drastically decreases at high temperatures, resulting in intensive aggregation. Moreover, high concentrations of protein may also lead to difficulties arising from aggregation of the denatured protein or, possibly, self-association of the native state. SPCI presented a tendency to form aggregates at high concentration of protein and at pH

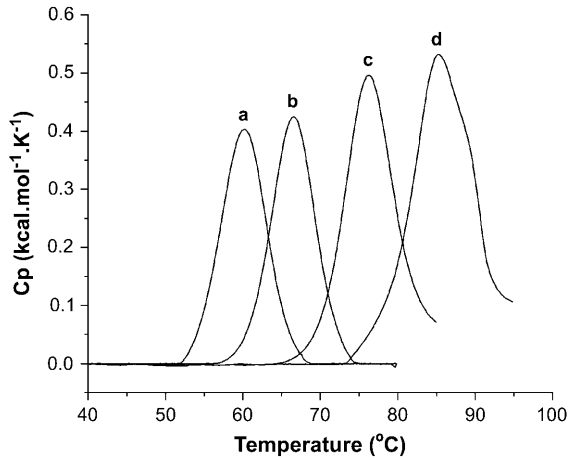

FIGURE 4 Profiles of heat-dependent unfolding of SPCI monitored by DSC under these different pH conditions: (*a*) pH 2.0, (*b*) pH 2.5, (*c*) pH 3.0, and (*d*) pH 7.0. Thermodynamic parameters calculated from these isotherms are summarized in Table 2.

7.0 (Leite et al., 2002), as also shown by the DSC method at high temperature and at pH 7.0. This feature was not observed in the spectroscopy assays due to the low concentration of the SPCI. Despite that, and considering the reversibility of ~95% at pH 7.0, the isotherm was well fitted and centered at a transition temperature of 85.3°C with a calorimetric transition enthalpy change of 144.0 kcal mol^{-1}. The thermodynamic parameters obtained under neutral condition indicate a remarkable stability of SPCI in which T_m occurs at a high temperature of 85.3°C, in agreement with most mesophilic and thermophilic globular proteins (Kumar et al., 2000, 2001), human lysozyme, parvalbumin, RNase T_1, and whale myoglobin (Robertson and Murphy, 1997).

The thermal stability of SPCI was also characterized as a function of acid pH by DSC (Fig. 4) and these results are summarized in Table 2. No change in shape of the SPCI rescanned thermograms was observed when the pH was varied between 2.0 and 5.0 indicating that the thermal unfolding at all acidic pH was totally reversible. Therefore, these transition curves can be described as single cooperative endotherms analyzed using a two-state model in which only the native and unfolded proteins are populated. As can be seen in Table 2, the transition temperature depends on the pH, varying from 57°C at pH 2.0–80.0°C at pH 5.0. A direct comparison of the denaturation parameters shows little difference in thermal stability at acid (pH = 5.0) or neutral pH. The maximum values for T_m, 80.0 and 85.3°C, and enthalpy change, 134.1 kcal mol^{-1} and 144.0 kcal mol^{-1}, occur at pH 5.0 and 7.0, respectively (Table 2). Comparison of the neutral and alkaline pH states from CD spectra reveals slight differences in the thermal stability, but at acidic pH of 3.0, below the *pI*, a significant difference in thermal stability was observed (Tables 1 and 2). It is well established that the maximum stability of a globular protein occurs near its *pI* (Pace, 1990; Dill, 1990; Staniforth et al., 1998). However, analyses of CD spectra of SPCI at pH 4.2, near its *pI* of 4.4 suggest an increase in stability with similar thermodynamic parameters obtained at pH 7.0: T_m of 85°C, ΔH_m of ~165 kcal mol^{-1}, and ΔG^{25} of ~18–20 kcal mol^{-1}. Despite these small differences in stability, a pH-dependence of the denaturation temperature of SPCI was detected revealing a broad maximum at pH ranging from 4.2 to 8.8, but the maximum stability coinciding with neutral, and at pH near its isoelectric point of 4.4. The maximum conformational stability of SPCI at zero net charge could be due to the favorable electrostatic interactions among the positive and negative charged groups arranged on the surface of protein as a consequence of decreasing the surrounding effective dielectric constant. However, although the thermodynamic parameters calculated from CD spectra at pH 4.2 have suggested a high stability of SPCI, the measurement of other transition curves slightly far from the isoelectric point are needed to prevent aggregation at posttransition baseline to conclude anything about the stability of SPCI in this condition.

TABLE 2 Thermodynamic parameters for the thermal unfolding of SPCI by DSC scan at different pH values

pH*	T_m (°C)	ΔH_{cal} (kcal mol^{-1})	ΔG^{25} (kcal mol^{-1})
2.00	57.0	95.7	6.5
2.25	60.0	104.0	7.7
2.50	64.0	100.0	7.6
2.75	69.5	117.0	10.0
3.00	72.0	121.0	10.6
3.20	76.0	128.0	12.0
5.00	80.0	134.1	13.3
7.00	85.3	144.0	15.1

*The estimated errors of the parameters are small, usually <2%.

The decrease in stability was observed at pH < 2.75 and the maximum stability of SPCI occurs at pH > 3.0. The decrease in transition temperatures and the enthalpy changes, during acidification at pH below 2.75 (Fig. 4 and Table 2), most likely is the result of the disruption of the electrostatic interactions and differences in *pK* values of negative and positive charged groups flatting during the unfolded transition at different pH values. As previously reported, the high ionic strength affects the inhibitory activity of SPCI by reducing the electrostatic interactions as a consequence of the dielectric constant increase (Souza et al., 2000).

As shown in Tables 1 and 2, small differences were found for the thermodynamic parameters obtained from the analyses of the calorimetric and spectroscopic data. ΔH_{cal} (144.0 kcal mol^{-1}) and ΔG^{25} (15.1 kcal mol^{-1}) measured calorimetrically at pH 7.0 were similar to those measured spectroscopically by CD and fluorescence combined data (ΔH_m of 145.0 ± 6 kcal mol^{-1} and ΔG^{25} of 15.4 ± 2.1 kcal mol^{-1}) but somewhat slightly different from the values measured by CD or fluorescence. The differences between thermodynamic parameters calculated from direct calorimetric and indirect equilibrium processes estimating the protein stability have been discussed in the literature (Makhatadze and Privalov, 1992; Sinha et al., 2000). Nonnative states of the protein that may be undistinguishable by CD and fluorescence could contribute differently to enthalpy and the heat capacity of the system. The two following reasons appear to be responsible for these differences: DSC provides a direct estimation of the denaturation enthalpy change and the constant-pressure heat-capacity change, whereas in the spectroscopic methods the thermodynamic parameters are estimated from the equilibrium constants evaluated from the denaturant-induced conformational-transition curves representing the equilibrium between the native and the unfolded states. Furthermore, whereas CD and fluorescence spectroscopy are sensitive to the disruption of the native structure upon unfolding, DSC monitors the heat capacity of the protein whatever its state.

The most common method for the determination of ΔC_p of a protein is the measurement of its heat-induced unfolding at different pH values (Privalov, 1979; Becktel and Shellman, 1987), assuming that ΔC_p does not depend on pH and temperature (Swint and Robertson, 1993; Pace and Laurent, 1989; Makhatadze, 1998; Pace et al., 1999). Fig. 5 shows

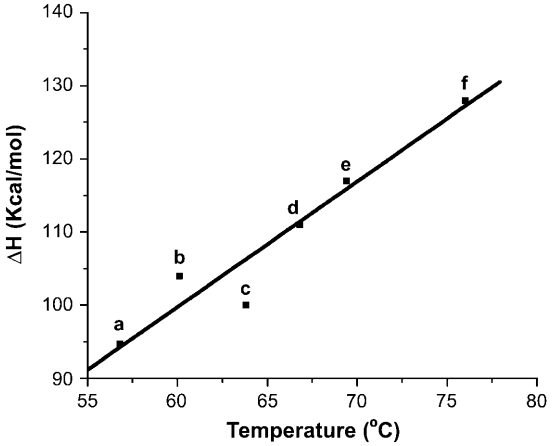

FIGURE 5 Dependence of the enthalpy change of SPCI unfolding on T_m at different pH values. (*a*) pH 2.00, (*b*) pH 2.25, (*c*) pH 2.50, (*d*) pH 2.75, (*e*) pH 3.00, and (*f*) pH 3.20. The slope of the line represents the heat-capacity change upon unfolding, $\Delta C_p = 1.72 \pm 0.24$ kcal mol^{-1} K^{-1}.

a linear relation between ΔH_m and T_m for SPCI producing a ΔC_p value of 1.72 ± 0.24 kcal mol^{-1} K^{-1} from the slope of the fitted curve. The change in specific heat ΔC_p at different acidic conditions reveals the independence of this thermodynamic parameter with respect to the temperature.

The conformational stability of SPCI expressed in terms of ΔG^{25} over a wide range of temperature and pH 3.0, 5.0, and 7.0, described by the Gibbs-Helmholtz relation (Eq. 6), is presented in Fig. 6. The temperatures of the maximum stabilities T_{max} derived from the analysis of those curves were 12°C, in agreement with those estimated from CD spectra, and the corresponding ΔG_{max} were 11.6 kcal mol^{-1} (pH 3.0), 13.9 kcal mol^{-1} (pH 5.0), and 15.7 kcal mol^{-1} (pH 7.0). Small differences in pH result in slight changes in T_m and in the corresponding stability ΔG^{25}, but no significant change in T_{max}. It must be noted that small differences in ΔH_m will result in relatively large changes in ΔG^{25} at pH $<$ 3.0 (Tables 1 and 2). Overall, the much higher value of ΔH_m reflects a higher ΔG^{25} given by the Gibbs-Helmholtz relationship. For SPCI, these values are relatively high compared to other small globular proteins (Privalov and Gill, 1988; Privalov, 1990; Robertson and Murphy, 1997), again demonstrating its high thermal stability under a broad range from acidic to alkaline conditions.

The transition curves obtained by calorimetry and the combined fluorescence and CD data at pH 7.0 (Fig. 7) are almost coincident, suggesting that the system is in thermodynamic equilibrium (Sturtevant, 1987) and that the unfolding transition observed in all techniques is probably the same and involves two states at pH 7.0 (Privalov, 1979). The inset of Fig. 7 shows the difference between the fluorescence and CD experimental points and the calculated curve from calorimetric parameters; the maxima difference is in the order of ± 0.05 units, reinforcing the agreement between the experimental data obtained by three different techniques. The differences in thermodynamic parameters at pH 7.0 between the two spectroscopic techniques only highlight the experimental difficulty of assessing these values of highly cooperative transitions.

CONCLUSIONS

The temperature of maximum stability (T_{max}), the corresponding free energy (ΔG_{max}), and the temperature-dependent calorimetric and spectroscopic measurements indicate that intact SPCI exhibits significant conformational and thermal stability from pH 3.0 to 8.8. Additionally, DSC profile analysis reveals endotherms that are characterized by a transition temperature and an unfolding enthalpy related to groups

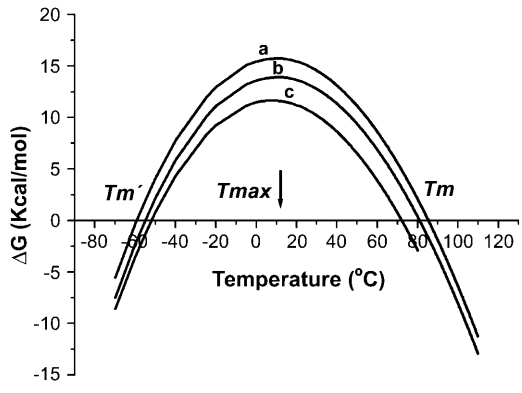

FIGURE 6 Gibbs-Helmholtz free-energy change as a function of temperature for the unfolding of SPCI at pH 7.0 (*a*), pH 5.0 (*b*), and pH 3.0 (*c*) obtained by DSC. The solid curves were calculated with Eq. 6 (see Materials and Methods) using T_m and ΔH_{cal} from isotherms and ΔC_p from the curve presented in Fig. 5. The corresponding stabilities were pH dependent (ΔG of 11.6 kcal mol^{-1} at pH 3.0, 13.9 kcal mol^{-1} at pH 5.0, and 15.7 kcal mol^{-1} at pH 7.0) and $T_{max} = 12$°C.

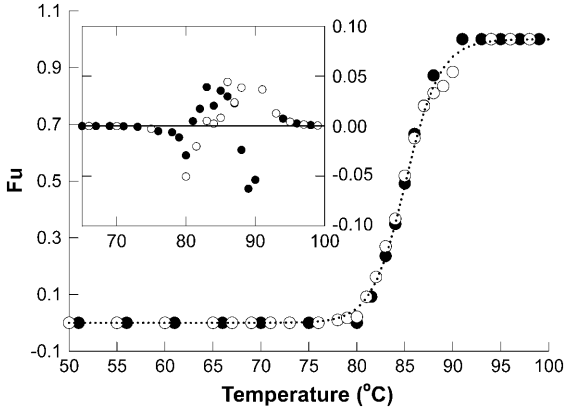

FIGURE 7 Plot of degree of denaturation (F_u) versus temperature of the combined calorimetric, circular dichroism, and fluorescence data at pH 7.0. The estimated thermodynamic parameters derived from these analyses are presented in Tables 1 and 2. Fluorescence data (*open circles*); CD data (*solid circles*); calculated curve from calorimetric parameters (*dashed line*). (*Inset*) Difference between the fluorescence and CD experimental points and the calculated curve from calorimetric parameters.

of highly stable proteins. Temperature-dependent far-UV CD studies showed discrete changes in which the neutral pH state exhibits a transition midpoint that is characterized by a decrease in molar ellipticity with disruption of ~70% of the secondary structure at a transition temperature of 84.9°C. The remarkable agreement between the T_m and ΔH values measured by the three independent techniques indicates that the system remains in thermodynamic equilibrium during the time in which the thermal unfolding occurs.

The thermal denaturation of SPCI can be well described as a two-state model in which intermediates with an enthalpy other than that of the unfolded protein are not populated at equilibrium. This conclusion comes from the following evidences: a), the unfolding data can be fitted to a single transition curve; b), the ratio of the van't Hoff enthalpy change of denaturation to the calorimetric enthalpy change obtained using DSC or spectroscopic methods is close to unity; and c), the remarkable agreement between the fitted transition curves and van't Hoff plot obtained by CD and fluorescence spectroscopy and calorimetry.

Finally, we conclude that all thermodynamic parameters obtained from fluorescence, CD, and DSC measurements strongly suggest that the thermal stability of SPCI in the native state is found in the upper end of the range observed for globular proteins. SPCI has an unusual thermostability with highest values of Gibbs free energy at a range of pH of 2.0–7.0 (6.5–15.4 kcal mol^{-1}) and enthalpy change of 95–145 kcal mol^{-1} in agreement with human lysozyme, parvalbumin, RNase T_1, and whale myoglobin (Robertson and Murphy, 1997). The three-dimensional structure of SPCI was not solved to allow the recognition of the electrostatic interactions, the chemical basis, and the mechanistic origin that would explain its high stability. However, this study suggests that this feature may be attributed to the self-association tendency and the possible high number of ionic pairs. These results are in accordance to previous reports indicating that the native structure of SPCI is mainly maintained by hydrophobic forces and electrostatic interactions (Souza et al., 2000; Leite et al., 2002). Thermodynamic analysis using all these methods reveals that SPCI is thermally a highly stable protein, over a wide range of pH 3.0–8.8, exhibiting maximum stability in the region ranging from 5.0 to 8.8. The structural arrangement of the charged groups in the three-dimensional structure of SPCI is not known. However, the low histidine content of SPCI (~1.7%) suggests flat pH dependence in the region 5.0–8.8. The decrease in stability at low pH can be due the differences in *pK* values of the acid groups (~22.5%) in the folded and unfolded states reflecting higher H^+ binding affinity of acidic residues in the unfolded state relative to the native state.

This work was supported by Conselho Nacional de Desenvolvimento Científico e Tecnológico (CNPq), Coordenação de Aperfeiçoamento de Pessoal de Nível Superior (CAPES), Fundação de Empreendimentos Científicos e Tecnológicos (FINATEC), and Brazilian Synchrotron Light Laboratory (LNLS-Brazil)/National Structural Molecular Biology program (RENABIME).

REFERENCES

Arnold, U., and R. Ulbrich-Hofmann. 1997. Kinetic and thermodynamic thermal stabilities of ribonuclease A and ribonuclease B. *Biochemistry.* 36:2166–2172.

Ascenzi, P., A. Bocedi, M. Bolognesi, A. Spallarossa, M. Colleta, R. De Cristofaro, and E. Menegatti. 2003. The bovine basic pancreatic trypsin inhibitor (Kunitz inhibitor): a milestone protein. *Curr. Protein Pept. Sci.* 4:231–251.

Becktel, W. J., and J. A. Shellman. 1987. Protein stability curves. *Biopolymers.* 26:1859–1877.

Bode, W., and R. Huber. 2000. Structural basis of the endoproteinase-protein inhibitor interaction. *Biochim. Biophys. Acta.* 1477:241–252.

Bolotina, I. A. 1987. Determination of protein secondary structure by circular-dichroism spectra. 5. The secondary structure of proteins in molten globule state. *Mol. Biol. (Mosk.).* 21:1625–1635.

Bolotina, I. A., and V. I. Lugauskas. 1985. Determination of the secondary structure of proteins from the circular-dichroism spectra. 4. Consideration of the contribution of aromatic amino-acid-residues to the circular-dichroism spectra of proteins in the peptide region. *Mol. Biol. (Mosk.).* 19:1409–1421.

Bown, D. P., H. S. Wilkinson, and J. A. Gatehouse. 1997. Differentially regulated inhibitor sensitive and insensitive protease genes from phytophagous insect pest. Heliocoverpa armigera are members of complex multigene families. *Insect Biochem. Mol. Biol.* 27:625–638.

Broadway, R. M. 1995. Are insects resistant to plant proteinase-inhibitors? *J. Insect Physiol.* 41:107–116.

Burova, T. V., E. P. Varfolomeeva, V. Y. Grinberg, T. Haertle, and V. B. Tolstoguzov. 2002. Effect of polysaccharides on the stability and renaturation of soybean trypsin (Kunitz) inhibitor. *Macromol. Biosci.* 2: 286–292.

Dill, K. A. 1990. Dominant forces in protein folding. *Biochemistry.* 29: 7133–7155.

Eftink, M. R. 1994. The use of fluorescence methods to monitor unfolding transitions in proteins. *Biophys. J.* 66:482–501.

Eftink, M. R., and M. C. Shastry. 1997. Fluorescence methods for studying kinetics of protein-folding reactions. *Methods Enzymol.* 278:258–286.

Franco, O. L., R. C. Santos, J. A. N. Batista, A. C. M. Mendes, M. A. M. Araújo, R. G. Monnerat, M. F. G. DeSá, and S. M. Freitas. 2003. Effects of black-eyed pea trypsin inhibitor on proteolytic activity and on development of *Anthonomous grandis*. *Phytochemistry.* 63:343–349.

Ganesh, C., N. Eswar, S. Srivastava, C. Ramakrishnan, and R. Varadarajan. 1999. Prediction of the maximal stability temperature of monomeric globular proteins solely from amino acid sequence. *FEBS Lett.* 454: 31–36.

Grinberg, V. Y., T. V. Burova, T. Haertl, and V. B. Tolstoguzov. 2000. Interpretation of DSC data on protein denaturation complicated by kinetic and irreversible effects. *J. Biotechnol.* 79:269–280.

Hilder, V. A., and D. Boulter. 1999. Genetic engineering of crop plants for insect resistance: a critical review. *Crop Prot.* 18:177–191.

Joshi, B., M. Sainani, K. Bastawade, V. S. Gupta, and P. K. Ranjekar. 1998. Cyteine protease inhibitor from pearl millet: a new class of antifungal protein. *Biochem. Biophys. Res. Commun.* 246:382–387.

Kobayashi, H., M. Suzuki, N. Kanyama, and T. Terao. 2004. A soybean Kunitz trypsin inhibitor suppresses ovarian cancer cell invasion by blocking urokinase upregulation. *Clin. Exp. Metastasis.* 21:159–166.

Kumar, S., C. J. Tsai, and R. Nussinov. 2000. Factors enhancing protein thermo stability. *Protein Eng.* 13:179–191.

Kumar, S., C. J. Tsai, and R. Nussinov. 2001. Thermodynamic differences among homologous thermophilic and mesophilic proteins. *Biochemistry.* 40:14152–14165.

Kumar, S., C. J. Tsai, and R. Nussinov. 2003. Maximal stabilities of reversible two-state proteins. *Biochemistry.* 42:4864–4873.

Laskowski, M., and I. Kato. 1980. Protein inhibitors of proteinase. *Annu. Rev. Biochem.* 49:593–626.

Laskowski, M., Jr., and M. A. Qasim. 2000. What can the structures of enzyme-inhibitor complexes tell us about the structures of enzyme-substrate complexes? *Biochim. Biophys. Acta.* 1477:324–337.

Leite, J. R. S. A., L. P. Silva, C. C. Taveira, R. C. L. Teles, S. M. Freitas, and R. B. Azevedo. 2002. Topographical analysis of *Schizolobium parahyba* chymotrypsin inhibitor (SPCI) by atomic force microscopy. *Protein Pept. Lett.* 9:179–185.

Makhatadze, G. I. 1998. Heat capacities of amino acids, peptides and proteins. *Biophys. Chem.* 71:133–156.

Makhatadze, G. I., K. Kim, C. Woodward, and P. L. Privalov. 1993. Thermodynamics of BPTI folding. *Protein Sci.* 2:2028–2036.

Makhatadze, G. I., and P. L. Privalov. 1992. Protein interactions with urea and guanidinium chloride. A calorimetric study. *J. Mol. Biol.* 226: 491–510.

Otlewski, J., M. Jaskolski, O. Buczek, T. Cierpicki, H. Czapinska, D. Krowarsch, A. O. Smalas, D. Stachowiak, A. Szpineta, and M. Dadlez. 2001. Structure-function relationship of serine protease-protein inhibitor interaction. *Acta Biochim. Pol.* 48:419–428.

Otlewski, J., D. Krowarsch, and W. Apostoluk. 1999. Protein inhibitors of serine proteinases. *Acta Biochim. Pol.* 46:531–565.

Pace, C. N. 1990. Conformational stability of globular proteins. *Trends Biochem. Sci.* 15:14–17.

Pace, N. C., G. R. Grimsley, S. T. Thomas, and G. I. Makhatadze. 1999. Heat capacity changes for ribonuclease A folding. *Protein Sci.* 8: 1500–1504.

Pace, C. N., and D. V. Laurent. 1989. A new method for determining the heat-capacity change form protein folding. *Biochemistry.* 28:2520–2525.

Pritchard, L., and M. J. Dufton. 1999. Evolutionary trace analysis of the Kunitz/BPTI family of proteins: functional divergence may have been based on conformational adjustment. *J. Mol. Biol.* 285:1589–1607.

Privalov, P. L. 1979. Stability of proteins: small globular proteins. *Adv. Protein Chem.* 33:167–241.

Privalov, P. L. 1990. Cold denaturation of proteins. *Crit. Rev. Biochem. Mol. Biol.* 25:281–305.

Privalov, P. L., and S. J. Gill. 1988. Stability of protein structure and hydrophobic interaction. *Adv. Protein Chem.* 39:191–234.

Privalov, P. L., and G. I. Makhatadze. 1992. Contribution of hydration and non-covalent interactions to the heat capacity effect on protein unfolding. *J. Mol. Biol.* 224:715–723.

Privalov, P. L., and G. I. Makhatadze. 1993. Contribution of hydration to protein folding thermodynamics. II. The entropy and Gibbs energy of hydration. *J. Mol. Biol.* 232:660–679.

Privalov, P. L., and S. A. Potekhin. 1986. Scanning microcalorimetry in studying temperature-induced changes in proteins. *Methods Enzymol.* 131:4–51.

Ptitsyn, O. B., and V. N. Uversky. 1994. The molten globule is 3D thermodynamically state of protein molecules. *FEBS Lett.* 341:15–18.

Richardson, M. 1977. The proteinase inhibitor of plants and microorganism. *Phytochemistry.* 16:159–169.

Richardson, J. M., S. D. Lemaire, J. P. Jacquot, and G. I. Makhadze. 2000. Difference in the mechanisms of the cold and heat induced unfolding of thioredoxin from *Chlamydomonas reinhardtii*: spectroscopic and calorimetric studies. *Biochemistry.* 39:11154–11162.

Robertson, A. D., and K. P. Murphy. 1997. Protein structure and the energetics of protein stability. *Chem. Rev.* 97:1251–1267.

Ryan, C. A. 1990. Protease inhibitors in plants: genes for improving defenses against insects and pathogens. *Annu. Rev. Phytopathol.* 28: 425–449.

Santoro, M. M., and D. W. Bolen. 1992. A test of the linear extrapolation of unfolding free energy changes over an extended denaturant concentration range. *Biochemistry.* 31:4901–4907.

Schuler, H. T., M. G. Poppy, and L. Denholm. 1998. Insect-resistant transgenic plants. *Trends Biotechnol.* 16:168–174.

Shukle, R. H., and L. Wu. 2003. The role of protease inhibitors and parasitoids on the population dynamics of *Sitotroga cerealella* (Lepidoptera: Gelechiidae). *Environ. Entomol.* 32:488–498.

Sinha, A., S. Yadav, R. Ahmad, and F. Ahmad. 2000. A possible origin of differences between calorimetric and equilibrium estimates of stability parameters of proteins. *Biochem. J.* 345:711–717.

Souza, E. M. T., K. Mizuta, M. U. Sampaio, and C. M. Sampaio. 1995. Purification and partial characterization of a S*chizolobium parahyba* chymotrypsin inhibitor. *Phytochemistry.* 39:521–525.

Souza, E. M. T., R. C. L. Teles, E. M. A. Siqueira, and S. M. Freitas. 2000. Effects of denaturing and stabilizing agents on the inhibitory activity and conformational stability of *Schizolobium parahyba* chymotrypsin inhibitor. *J. Protein Chem.* 9:507–513.

Staniforth, R. A., M. G. Bigotti, F. Cutruzzola, C. T. Allocatelli, and M. Brunori. 1998. Unfolding of apomyoglobin from *Aplysia limacina*: the effect of salt and on the cooperativity of folding. *J. Mol. Biol.* 275: 133–148.

Sturtevant, J. M. 1987. Biochemical applications of differential scanning calorimetry. *Annu. Rev. Phys. Chem.* 38:463–488.

Swint, L., and A. D. Robertson. 1993. Thermodynamics of unfolding for turkey ovomucoid third domain: thermal and chemical denaturation. *Protein Sci.* 2:2037–2049.

Teles, R. C. L., S. M. Freitas, Y. Kawano, E. M. T. Souza, and E. P. G. Áreas. 1999. Vibrational spectroscopic analysis of a chymotrypsin inhibitor isolated from *Schizolobium parahyba* (Vell) Toledo seeds. *Spectrochimica Acta Part A.* 55:1279–1289.

Teles, R. C. L., E. M. T. Souza, L. A. Calderon, and S. M. Freitas. 2004. Purification and pH stability characterization of a chymotrypsin inhibitor from *Schizolobium parahyba* seeds. *Phytochemistry.* 65:793–799.

Tsonev, L. I., and A. G. Hirsh. 2000. Fluorescence ratio intrinsic basis states analysis: a novel approach to monitor and analyze protein unfolding by fluorescence. *J. Biochem. Biophys. Methods.* 45:1–21.

Valueva, T. A., and V. V. Mosolov. 1999. Protein inhibitors of proteinases in seeds. 1. Classification, distribution, structure, and properties. *Russ. J. Plant Physiol.* 46:307–321.

Varfolomeeva, E. P., T. V. Burova, V. Y. Grinberg, and V. B. Tolstoguzov. 1989. Thermodynamic and kinetic-study of thermal-denaturation of the Kunitz trypsin-inhibitor from soybean by differential scanning microcalorimetry. *Mol. Biol. (Mosk.).* 23:1263–1272.

Venyaminov, S. Y., S. Yu, and J. T. Yang. 1996. Determination of protein secondary structure. *In* Circular Dichroism and the Conformational Analysis of Bio-Macromolecules. G. D. Fasman, editor. Plenum Press, New York. 69–107.

Wilson, K. A., and J. C. Chen. 1983. Amino acid sequence of mung bean trypsin inhibitors and its modified form appearing during germination. *Plant Physiol.* 71:341–349.

Yang, J. T., C. S. C. Wu, and H. M. Martinez. 1986. Calculation of protein conformation from circular-dichroism. *Methods Enzymol.* 30:208–269.

Zweifel, M. E., and D. Barrick. 2002. Relationships between the temperature dependence of solvent denaturation and the denaturant dependence of protein stability curves. *Biophys. Chem.* 101:221–237.